# The circular capillary jump

**Rajesh K. Bhagat†, and P. F. Linden,**

Department of Applied Mathematics and Theoretical Physics,
Wilberforce Road, Cambridge CB3 0WA, UK

(Received xx; revised xx; accepted xx)

In this paper we re-examine the flow produced by the normal impact of a laminar liquid jet onto an infinite plane when the flow is dominated by surface tension. It is observed experimentally that after impact the liquid spreads radially over the plane away from the point of impact in a thin film. It is also observed that, at a finite radius, there is an abrupt increase in thickness of the film which has been identified as a hydraulic jump, and that this radius is independent of the orientation of the surface showing that gravity is unimportant (Bhagat *et al.* 2018). We show that the application of conservation of momentum in the film, subject only to viscosity and surface tension and ignoring gravity completely, predicts a singularity in the curvature of the liquid film and consequently a jump in the depth of the film at a finite radius. This location is almost identical to the radius of the jump predicted by conservation of energy and agrees with experimental observations.

## 1. Introduction

In a recent paper Bhagat *et al.* (2018) conducted experiments which showed that in a thin liquid film, on scales typical of those found in a kitchen sink, the circular jump produced by the normal impact of a round laminar jet onto an infinite plane is independent of the orientation of the surface. These experiments conclusively showed that gravity does *not* play a significant role in the formation of these jumps – in sharp contrast with previous theoretical analyses. They also used conservation of energy, including both surface tension *and* gravity, to determine the radius of the jump. As we discuss below, on the scale of a kitchen sink the predicted radius is found to be almost independent of gravity, and is in excellent agreement with the experiments, which cover fluids with a range of surface tension values.

Conventionally the circular hydraulic jump has been studied in an experimental setup where a vertical jet impinges on a horizontal disk and either flows over a weir or off the edge of the plate. In this paper we are concerned with the situation in which the plate is sufficiently large so that the jump forms before the spreading liquid film encounters either the weir or the edge (figure 1(a)). Once the film reaches the edge of the plate a different boundary condition is imposed that changes the depth of the subcritical film, which, in turn, changes the position of the previously-formed jump. Usually, in this later adjustment, since the subcritical region is signficantly deeper than the supercritical region upstream of the jump, gravity plays a significant role. Consequently, since the influence of the plate-edge condition was important in experiments many previous studies (Bohr *et al.* 1993; Liu & Lienhard 1993; Bush & Aristoff 2003; Kasimov 2008; Mathur *et al.* 2007; Rojas *et al.* 2010) concluded that gravity was the dominant force in the jump formation.

On the other hand, Mohajer & Li (2015) (see their figures 4 and 13) measured the

† Email address for correspondence: rkb29@cam.ac.uk

jump radius and the height of the liquid downstream of the jump for water and a water-surfactant solution. They observed a significant increase in the jump radius when the surface tension was reduced. They also reported that for a range of flow rates the jump height remained constant and depended only on the surface tension of the liquid. These experiments suggested that surface tension was the dominant force. This was later conclusively confirmed by our experiments on plates a different orientations (Bhagat *et al.* 2018).

We first consider the implications of dimensional analysis. The relative importance of gravity $g$ and surface tension $\gamma$ depends on the fluid properties, density $\rho$ and kinematic viscosity $\nu$, and the flow characterised by the jet flow rate $Q$. Dimensional analysis shows that when gravity or surface tension is ignored the jump radius scales, respectively, as

$$R_{\mathrm{ST}} \sim \frac{Q^{3/4}\rho^{1/4}}{\nu^{1/4}\gamma^{1/4}} \text{ or } R_{\mathrm{G}} \sim \frac{Q^{5/8}}{\nu^{3/8}g^{1/8}}. \tag{1.1}$$

Consequently, the jump will either be caused by surface tension if $R_{\mathrm{ST}} < R_{\mathrm{G}}$ and *vice-versa*. This criterion leads to a critical flow rate $Q_{\mathrm{C}}$ given by

$$Q_{\mathrm{C}} = \frac{\gamma^2}{\nu\rho^2 g}, \tag{1.2}$$

below which surface tension is the dominant force and above which gravity is important. For water $Q_C \approx 500\,\mathrm{cm^3\,s^{-1}}$ (i.e. $\approx 30\,\mathrm{L\,min^{-1}}$) which is significantly faster than the flow in the standard kitchen sink. Table 1 gives values of $Q_C$ for liquids used in experiments (Bohr *et al.* 1993; Bhagat *et al.* 2018; Duchesne *et al.* 2019) and we see that $Q \ll Q_C$ in the experiments in water, and that the flow rates are only comparable in the experiments with ethylene glycol and silicone oil. In fact, as we show from a more detailed analysis in the Appendix, the jump is dominated by surface tension even when $Q \sim 10Q_C$.

Despite this conclusive experimental evidence, a new body of literature (Duchesne *et al.* (2019); Wang & Khayat (2019); Sen *et al.* (2019)) supports the previous gravity-based theory. In particular, Duchesne *et al.* (2019) appear to have ignored the experimental evidence and presented a theory, purporting to show surface tension does not play a significant role in the formation of the jump. It is clear, therefore, that there are still conflicting views on the dynamics responsible for these jumps. One objective of this paper is to clarify this confusion.

The other objective is to show that the jump radius can be predicted using momentum conservation and show that this is consistent with the energy-based approach used by Bhagat *et al.* (2018). In order to focus on the role of surface tension we predict the jump location using conservation of momentum, ignoring gravity completely. The paper is organised as follows. The role of surface tension at the liquid-gas interface in a flowing, as distinct from stationary, liquid is derived and applied to a radially spreading thin film in §2. Here we also discuss the force due to surface tension at jump location and compare it with Bush & Aristoff (2003)'s analysis. The application of conservation of momentum in both the radial and film-normal directions is given in §3. The energy based approach presented in Bhagat *et al.* (2018) is revisited and compared with the momentum based approach in §4. Here, we also re-visit the analysis of Duchesne *et al.* (2019). Finally, our conclusions are given in §5.

## 2. Theory

### 2.1. *Surface tension force*

Fluid motion is governed by the Navier-Stokes equations which express conservation of momentum in a fluid continuum. For flows with an interface between two fluids, the

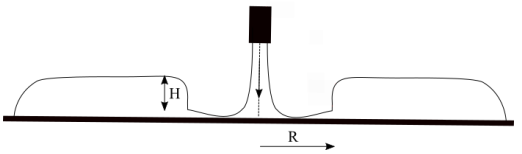


(a) Hydraulic jump on an infinite plate

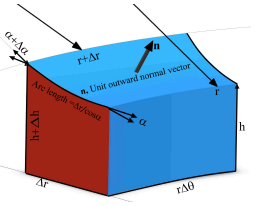


(b) Control volume

Figure 1: Hydraulic jumps on (a) an infinite flat plate where, as observed experimentally (Bhagat *et al.* 2018), the jump forms with no influence of a downstream boundary condition (b) schematic of the differential volume showing the slope of the thin liquid film

| Liquid | Reference | $Q$ | $Q_c$ | $\gamma \times 10^{-3}$ | $\nu \times 10^{-6}$ |
|---|---|---|---|---|---|
| | | ($\mathrm{cm^3\,s^{-1}}$) | ($\mathrm{cm^3\,s^{-1}}$) | ($\mathrm{kg\,s^{-2}}$) | ($\mathrm{m\,s^{-2}}$) |
| Water | Mohajer & Li (2015) | 2.5-8.33 | 518 | 72 | 1.002 |
| Ethylene glycol | Rojas *et al.* (2010) | 20 | 22 | 45 | 7.6 |
| Silicon oil - 1 | Duchesne *et al.* (2014) | 4.3-60 | 2.3 | 20 | 20 |
| Silicon oil - 2 | Duchesne *et al.* (2014) | - | 0.45 | 20 | 98 |
| WP95/5 | Bhagat *et al.* (2018) | 83-200 | 82 | 42.5 | 1.274 |
| WP80/20 | Bhagat *et al.* (2018) | 83-200 | 58 | 26 | 2.30 |
| SDBS | Bhagat *et al.* (2018) | 83-200 | 147 | 38 | 1 |

Table 1: Parameters used in published experiments. The jet flow rate $Q$, the critical flow rate $Q_C$ at which gravity begins to play a role, the surface tension $\gamma$, and the kinematic viscosity $\nu$ of the fluid.

Navier-Stokes equations do not express the surface tension force acting on the interface. This force is introduced as a normal stress boundary condition at the interface.

Consider a surface $S$, with unit normal $\mathbf{n}$, bounded by a closed contour $C$ with arc length $\mathbf{l}$, in the interface between two immiscible fluids, taken here to be the common case of a liquid and a gas denoted by the subscripts $L$ and $G$, respectively, with constant surface tension $\gamma$ (see figure 1(b)). Since the surface tension force acts in a direction perpendicular to $\mathbf{n}$ and the contour $C$, continuity of the normal stress is expressed as

$$\int_S (\mathbf{T}_G - \mathbf{T}_L) \cdot \mathbf{n} dS + \gamma \int_C d\mathbf{l} \times \mathbf{n} = 0, \tag{2.1}$$

where $\mathbf{T} = -p\mathbf{I} + \mu[\nabla\mathbf{u} + (\nabla\mathbf{u})^T]$ is the total stress, with pressure $p$ and velocity $\mathbf{u}$, and $\mu$ is the viscosity of the fluid.

Assuming the *dynamic* viscosity of the air is negligible compared to that of the liquid and denoting pressure in the air as $p_G$ and in the liquid as $p_L$, (2.1) can be written as

$$\int_S (-p_G + p_L)\mathbf{n} dS - \mu \int_S \mathbf{n}.[\nabla\mathbf{u} + (\nabla\mathbf{u})^T] dS + \gamma \int_C d\mathbf{l} \times \mathbf{n} = 0, \tag{2.2}$$

where $\mathbf{u}$ is the velocity in the liquid.

In the case of a stationary liquid and gas, the middle term of (2.2) is zero and this

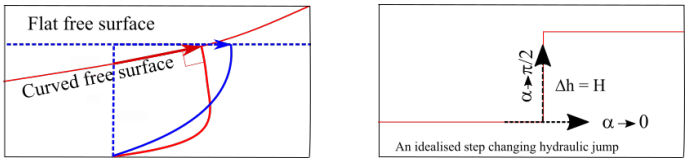


(a) Velocity profile (b) An idealised jump

Figure 2: (a) Schematic velocity profiles in a flow with conventional flat surface assumption with zero radial viscous stress (blue) and liquid interface with zero tangential stress but non-zero radial stress (red). The surface tension force retards the flow in the radial direction and accelerates it in the wall-normal direction, giving non-zero radial and wall-normal viscous stresses at the surface (2.1) (b) An idealised hydraulic jump.

equation gives the usual Laplace pressure in the liquid associated with the curvature of the surface. In the case of a flowing liquid the surface tension force can be balanced by the viscous stresses at the surface, and for a sufficiently fast flow this can be much larger than the Laplace pressure. Further, while the tangential stress at the free surface is zero, the curvature of the surface implies non-zero radial and wall-normal viscous stresses as shown in figure 2(a).

### 2.2. *Force on an axisymmetric thin film*

Following Bush & Aristoff (2003), for an axisymmetric thin film on a planar surface we write the equation of the surface in implicit form

$$J(r,z) = z - h(r) = 0, \tag{2.3}$$

which yields the vector normal to the film surface

$$\mathbf{n} = \frac{\nabla J}{|\nabla J|} = \frac{\hat{\mathbf{z}} - h'\hat{\mathbf{r}}}{(1+h'^2)^{1/2}}, \tag{2.4}$$

where $\hat{\mathbf{r}}$ and $\hat{\mathbf{z}}$ are unit vectors in the radial and wall-normal directions, respectively, and $h' = dh/dr$. We define the angle $\alpha$ as the tangent to the surface defined by $h' = \tan\alpha$. Then $\cos\alpha = \frac{1}{(1+(h'^2)^{1/2}}$ and $\sin\alpha = \frac{h'}{(1+h'^2)^{1/2}}$, and (2.4) can also be written as

$$\mathbf{n} = \hat{\mathbf{z}}\cos\alpha - \hat{\mathbf{r}}\sin\alpha. \tag{2.5}$$

For the control volume shown in figure 1(b), with the interface bounded by the closed contour $C$, the differential arc length $\Delta\mathbf{l} = (r\Delta\theta)\,\hat{\theta}\Big|_r^{r+\Delta r} - (\Delta r)\,\hat{\mathbf{r}}\Big|_\theta^{\theta+\Delta\theta} - (\Delta h)\,\hat{\mathbf{z}}\Big|_\theta^{\theta+\Delta\theta}$. Consequently, the force due to surface tension on this interface is

$$\Delta F_\gamma = \gamma\,(\Delta\mathbf{l}\times\mathbf{n}) = \gamma\,(\Delta\theta r\cos\alpha\hat{\mathbf{r}})\Big|_r^{r+\Delta r} + \gamma\,(\Delta\theta r\sin\alpha\hat{\mathbf{z}})\Big|_r^{r+\Delta r} + \gamma\left(\frac{\Delta r}{\cos\alpha}\hat{\theta}\right)\Big|_\theta^{\theta+\Delta\theta} \tag{2.6}$$

Considering the circular symmetry, in the limit of $\Delta r$ and $\Delta\theta \to 0$

$$dF_\gamma = \left(\gamma d(r\cos\alpha) - \gamma\frac{dr}{\cos\alpha}\right)d\theta\hat{\mathbf{r}} + \gamma d(r\sin\alpha)d\theta\hat{\mathbf{z}}. \tag{2.7}$$

We now revisit equation (2.1) noting that $S$ is an arbitrary surface and surface tension of the liquid is a constant, and using a vector identity and $\int_C \mathbf{n}\times d\mathbf{l} = -\int_S \gamma(\nabla_s\cdot\mathbf{n})\mathbf{n}ds$, to obtain an alternative form of the dynamic boundary condition

$$(\mathbf{T}_G - \mathbf{T}_L)\cdot\mathbf{n} = \gamma(\nabla_s\cdot\mathbf{n})\mathbf{n}, \tag{2.8}$$

where $\nabla_s = [\mathbf{I}-\mathbf{nn}].\nabla$ is the surface gradient, relating the jump in the normal stress to the curvature of the surface. Since (2.7) is equivalent to $-(\nabla.\mathbf{n})\mathbf{n}ds$ this is in agreement with the normal stress condition given in Bush & Aristoff (2003). Finally, from (2.2) and (2.7), the radial and vertical components of the normal stress at the free surface can be written as

$$\begin{aligned} F_{\gamma,r} \equiv \int_r^{r+\Delta r} \mu\left(\mathbf{n}\cdot[\nabla\mathbf{u}+(\nabla\mathbf{u})^T]\right)\cdot\hat{\mathbf{r}}\left(rd\theta\frac{dr}{\cos\alpha}\right)\Big|_h = \int_r^{r+\Delta r} P\sin\alpha r d\theta\frac{dr}{\cos\alpha} \\ +\gamma r d\theta\cos\alpha\Big|_r^{r+\Delta r} - \gamma\frac{\Delta r}{\cos\alpha}d\theta, \end{aligned} \tag{2.9}$$

and

$$F_{\gamma,z} \equiv \int_r^{r+\Delta r} \mu\left(\mathbf{n}\cdot[\nabla\mathbf{u}+(\nabla\mathbf{u})^T]\right)\cdot\hat{\mathbf{z}}\left(rd\theta\frac{dr}{\cos\alpha}\right)\Big|_h = \int_r^{r+\Delta r} Prd\theta dr + rd\theta\gamma\sin\alpha\Big|_r^{r+dr}, \tag{2.10}$$

where $P = p_L - p_G$. As we will see below, application of momentum conservation requires expressions for the radial gradients of these forces, and as axisymmetry implies we can drop $d\theta$, these are given by

$$\frac{dF_{\gamma,r}}{dr} = \frac{d}{dr}\left(\int_S \mu\left(\mathbf{n}\cdot[\nabla\mathbf{u}+(\nabla\mathbf{u})^T]\right)\cdot\hat{\mathbf{r}}\left(\frac{rdr}{\cos\alpha}\right)\Big|_h\right) = rP\tan\alpha - \frac{\gamma}{\cos\alpha} + \gamma\frac{d(r\cos\alpha)}{dr} \tag{2.11}$$

and

$$\frac{dF_{\gamma,z}}{dr} = \frac{d}{dr}\left(\int_r^{r+\Delta r} \mu\left(\mathbf{n}\cdot[\nabla\mathbf{u}+(\nabla\mathbf{u})^T]\right)\cdot\hat{\mathbf{z}}\left(\frac{rdr}{\cos\alpha}\right)\Big|_h\right) = rP + \gamma\frac{d(r\sin\alpha)}{dr}. \tag{2.12}$$

## 3. Momentum conservation

We now apply conservation of momentum to the axisymmetric flow spreading radially from the point of impact of the jet on the plane. In cylindrical coordinates with the origin at the point of jet impact let $u, w$ be the radial and vertical velocity components, respectively.

In order to determine the velocity field we assume, following Watson (1964), that the flow is self similar and that the radial velocity can be expressed as the product of the radially varying surface velocity $u_s(r)$ and a function of the similarity variable $\eta = z/h(r)$ in the form

$$u(r,z) = u_s(r)f(\eta), \quad \eta \equiv \frac{z}{h(r)},\ 0 \leqslant \eta \leqslant 1, \tag{3.1}$$

where $u_s$ is the surface velocity and $f(0) = 0, f(1) = 1$. Conservation of mass implies

$$\int_0^h urdz = ru_s h\int_0^1 f(\eta)d\eta \equiv C_1 u_s rh = \text{const.}, \tag{3.2}$$

and $C_1 \equiv \int_0^1 f(\eta)d\eta$ is an integration constant arising from the velocity profile . Incompressibility gives

$$w(\eta) = -\int_0^\eta \frac{1}{r}\frac{\partial ru}{\partial r}dz = -\frac{1}{r}\frac{d}{dr}[(ru_s h)\int_0^\eta f(\eta)d\eta].$$

Then, using (3.2)

$$w = -u_s h\frac{d}{dr}\int_0^\eta f(\eta)d\eta = uh'\eta = u_s h'\eta f(\eta), \tag{3.3}$$

which automatically satisfies the kinematic boundary conditions at the wall and interface. We now use these expressions for the velocity in equations expressing momentum conservation in the radial and wall-normal directions.

### 3.1. *Momentum balance in the radial direction*

In the absence of gravity, the momentum equation in the radial direction is

$$\rho\left(u\frac{\partial u}{\partial r} + w\frac{\partial u}{\partial z}\right) = \frac{1}{r}\frac{\partial(r\tau_{rr})}{\partial r} + \frac{\partial \tau_{rz}}{\partial z}, \tag{3.4}$$

where $\tau = \mathsf{T} + p\mathbf{I}$ is the deviatoric stress tensor (in cylindrical coordinates). Since the pressure in the gas at the surface is constant (atmospheric) and the film is thin, the radial pressure gradient in the liquid is only a function of radius caused by the curvature of the surface.

We use incompressibility ($\nabla \cdot \mathbf{u} = 0$), integrate (3.4) across the film from the wall to the interface, use axisymmetry to eliminate $d\theta$, substitute for the velocity from (3.1) and (3.3) and apply the surface tension boundary condition (2.11), to obtain

$$\frac{d}{dr}\int_0^h \rho r u^2 dz = -\int_0^h \frac{dp}{dr}rdz + rp\tan\alpha - \frac{\gamma}{\cos\alpha} + \gamma\frac{d(r\cos\alpha)}{dr} - \mu r\left(\frac{\partial u}{\partial z} + \frac{\partial w}{\partial r}\right)\Big|_0. \tag{3.5}$$

Noting that conservation of mass (3.2) implies $u_s rh = \text{const.}$ we obtain

$$C_2[\rho u_s rh\frac{du_s}{dr}] = -\frac{dp}{dr}rh + rp\tan\alpha - \frac{\gamma}{\cos\alpha} + \gamma\frac{d(r\cos\alpha)}{dr} - \mu r\left(\frac{\partial u}{\partial z} + \frac{\partial w}{\partial r}\right)\Big|_0, \tag{3.6}$$

where $C_2 = \int_0^1 f^2(\eta)d\eta$ is a second integration constant. Equation (3.6) can be written in terms of the interface slope

$$C_2[\rho u_s rh\frac{du_s}{dr}] = -\frac{dp}{dr}rh + rph' - \gamma(1+h'^2)^{1/2} + \gamma\frac{1}{(1+h'^2)^{1/2}} - \gamma\frac{rh'h''}{(1+h'^2)^{3/2}} - \tau_w r, \tag{3.7}$$

where $\tau_w = -\mu\left(\frac{\partial u}{\partial z} + \frac{\partial w}{\partial r}\right)\Big|_0$ is the wall shear stress.

### 3.2. *Momentum balance in wall-normal direction*

We now apply conservation of momentum in the wall-normal $z$ direction in the differential control volume shown in figure 1(c). Since the film is thin the pressure is independent of $z$ and for an axisymmetric flow

$$\rho u r\frac{\partial w}{\partial r}+\rho w r\frac{\partial w}{\partial z}=\frac{\partial(r\tau_{rz})}{\partial r}+r\frac{\partial \tau_{zz}}{\partial z}. \tag{3.8}$$

As before we integrate across the film to obtain

$$\int_0^h \rho u r\frac{\partial w}{\partial r}dz+\int_0^h \rho w r\frac{\partial w}{\partial z}dz=\int_0^h \frac{\partial(r\tau_{rz})}{\partial r}dz+2\mu\frac{\partial w}{\partial z}|^h. \tag{3.9}$$

Substituting for the velocity from (3.1) and (3.3), and applying the surface boundary condition (2.11) gives

$$\begin{aligned}\rho u_s r h\frac{d(u_s h')}{dr}\int_0^1 \eta f^2(\eta)d\eta-\rho h'^2 u_s^2 r\int_0^1 \eta f^2(\eta)d\eta-\rho\frac{u_s^2 r h'^2\eta^2 f^2(\eta)}{2}\Big|_0^1\\ +\rho h'^2 u_s^2 r\int_0^1 \eta f^2(\eta)d\eta+r\frac{\rho w^2}{2}\Big|_0^h=\frac{dF_{\gamma,z}}{dr}-\int\frac{\partial(r\tau_{rz})}{\partial r}dz\Big|_0+2\mu\frac{\partial w}{\partial z}|^h.\end{aligned} \tag{3.10}$$

Substituting (2.12) into (3.10) yields

$$\begin{aligned}\rho u_s r h\frac{d(u_s h')}{dr}\int_0^1 \eta f^2(\eta)d\eta&=rp+\gamma\frac{d(r\sin\alpha)}{dr}-\int\frac{\partial(r\tau_{rz})}{\partial r}dz\Big|_0+2\mu\frac{\partial w}{\partial z}|^h,\\ &=rp+\gamma r\sin\alpha+\gamma r\cos\alpha\frac{d\alpha}{dr}-\int\frac{\partial(r\tau_{rz})}{\partial r}dz\Big|_0+2\mu\frac{\partial w}{\partial z}|^h,\\ &=rp+\frac{\gamma r h'}{(1+h'^2)^{1/2}}+\frac{\gamma r h''}{(1+h'^{3/2})}-\int\frac{\partial(r\tau_{rz})}{\partial r}dz\Big|_0+2\mu\frac{\partial w}{\partial z}|^h.\end{aligned}$$

In the thin liquid film upstream of the hydraulic jump, the interface slope remains small and we will ignore the higher order terms in $\frac{dh}{dr}$. Applying this approximation and re-arranging (3.11) gives an expression for the curvature of the film

$$\begin{aligned}h''(\rho u_s^2 r h\int_0^1 \eta f^2(\eta)d\eta-\gamma r)+h'(\rho u_s r h\frac{du_s}{dr}\int_0^1 \eta f^2(\eta)d\eta-\gamma)=\\ rp-\int\frac{\partial(r\tau_{rz})}{\partial r}dz\Big|_0+2\mu\frac{\partial w}{\partial z}|^h.\end{aligned} \tag{3.11}$$

Finally, substituting $\rho u_s r h\frac{du_s}{dr}$ from the radial momentum balance (3.8) gives

$$\begin{aligned}[C_3\rho u_s^2 r h-\gamma r]h''+\frac{C_3}{C_2}h'(-\frac{dp}{dr}rh+rph'-\gamma(1+h'^2)^{1/2}+\gamma\frac{1}{(1+h'^2)^{1/2}}-\\ \gamma\frac{h'h''}{(1+h'^2)^{3/2}}-\tau_w r-\frac{C_2}{C_3}\gamma)=rp-\int\frac{\partial(r\tau_{rz})}{\partial r}dz\Big|_0+2\mu\frac{\partial w}{\partial z}|^h,\end{aligned} \tag{3.12}$$

where $C_3=\int_0^1 \eta f^2(\eta)d\eta$ is a third integration constant.

Ignoring higher order terms in $h'$ and re-arranging gives an expression for the curvature of the film

$$h''=\frac{-h'\frac{C_3}{C_2}[-\frac{dp}{dr}rh+r\tau_w-\frac{C_2}{C_3}\gamma]+rp+\int\frac{\partial(r\tau_{rz})}{\partial r}dz\Big|_0+2\mu\frac{\partial w}{\partial z}|^h}{C_3\rho u_s^2 r h(1-\mathrm{We}^{-1})} \tag{3.13}$$

where the Weber number $We$ is defined by

$$\mathrm{We}\equiv\frac{C_3\rho u_s^2 h}{\gamma}. \tag{3.14}$$

Consequently, we predict a singularity in the curvature of the film at a critical radius where the film thickness is such that $We = 1$. This criterion gives the location of the hydraulic jump.

### 3.3. *Revisiting the radial momentum balance*

In the previous section the momentum balance was confined inside the hydraulic jump radius where $h'$ is small. We now revisit the radial momentum balance (3.8) which can also be written as

$$C_2[\rho u_s r h du_s] = -rhdp + rpdh - \gamma(1+h'^2)^{1/2}dr + \gamma\frac{dr}{(1+h'^2)^{1/2}} - \gamma\frac{h'h''dr}{(1+h'^2)^{3/2}} - \tau_w r dr, \tag{3.15}$$

and apply it at the jump radius. We note that the jump is a singularity (see figure 2(b)), where $\frac{dh}{dr} = \tan\alpha \to \infty$, $\Delta r \to 0$, $\Delta h = H$ a finite quantity, and $\alpha$ changes from 0 to $\pi/2$. Substituting the trigonometric forms of the functions and integrating (3.15) at the jump location $r = R$ gives

$$\int C_2\rho u_s R h du_s = -\int Rhdp + \int Rpdh - \int \gamma\sin\alpha dh - \gamma R\cos\alpha\Big|_0^{\pi/2} + \int \gamma\cos\alpha dr - \int \tau_w R dr. \tag{3.16}$$

Then in scaled terms (3.16) can be written

$$C_2\rho {u_s}^2 Rh \approx RH(p - \frac{\gamma}{R}) + \gamma R. \tag{3.17}$$

Since at the jump the pressure $p$ scales as $\frac{\gamma}{R}$, the first term on the RHS of (3.17) is zero, which gives $We = 1$ as the condition for the hydraulic jump. Thus conservation of radial momentum gives the same result for the jump condition.

## 4. Relation to energy conservation

From (2.7) the energy flux associated with surface tension force on the control volume is

$$\Delta F_\gamma.(u\hat{\mathbf{r}} + w\hat{\mathbf{z}}) = \gamma\left(\Delta\theta u r\cos\alpha\right)\Big|_r^{r+\Delta r} + \gamma\left(\Delta\theta w r\sin\alpha\right)\Big|_r^{r+\Delta r}. \tag{4.1}$$

Circular symmetry implies that there is no net flux of fluid in the azimuthal direction and so substituting (3.3) into (4.1) yields

$$\gamma\left(\Delta\theta u r\cos\alpha\right)\Big|_r^{r+\Delta r} + \gamma\left(\Delta\theta w r\sin\alpha\right)\Big|_r^{r+\Delta r} = \gamma\left(\frac{\Delta\theta u r}{(1+h'^2)^{1/2}}\right)\Big|_r^{r+\Delta r} + \gamma\left(\frac{\Delta\theta u r h'^2}{(1+h'^2)^{1/2}}\right)\Big|_r^{r+\Delta r}. \tag{4.2}$$

Since upstream of the hydraulic jump the liquid film is almost flat we can ignore the higher order terms in $h'$ and, for an annular control volume, the energy flux is given by

$$2\pi r u\gamma\Big|_{r+\Delta r} - 2\pi r u\gamma\Big|_r. \tag{4.3}$$

Consequently, in a control volume approach the force due to surface tension, which appears through the normal stress boundary condition, can be incorporated as a surface force on the circumference of the control volume consistent with the analysis in Bhagat *et al.* (2018).

The normal stress boundary condition at the free surface also implies that the interior of the fluid experiences the effect of surface tension through a change in the velocity profile. Bhagat *et al.* (2018) did not consider this and used Watson's similarity velocity profile (Watson 1964) which assumed zero stress ($\frac{\partial u}{\partial z} = 0$) at the free surface. The surface velocity obtained using Watson's similarity velocity profile is, therefore, not the correct surface velocity (see figure 2(a)). Consequently, it is appropriate to associate the flux of surface energy with the average velocity rather than the surface velocity obtained from a boundary layer velocity profile.

We now return to the question of the the relative importance of gravity and surface tension in these flows. Duchesne *et al.* (2019) argued that the analysis of Bhagat *et al.* (2018) is wrong and that surface tension does not play a significant role in the formation in the hydraulic jump. Duchesne *et al.* (2019) wrote the energy equation in differential form as

$$\oint \left[ v_j \left( \frac{1}{2}\rho v^2 + p \right) - \mu v_i v_{i,j} \right] n_j dA - \frac{1}{2}\mu \int v_{i,j}^2 dV = 0. \tag{4.4}$$

However, Duchesne *et al.* (2019) only consider a part of (4.4), namely,

$$\chi(r) = \int_0^h u \left( \frac{1}{2}\rho(u^2 + w^2) + p \right) r dz \tag{4.5}$$

ignoring the term $\int_0^h \mu v_i v_{i,j} n_j dA$, which expresses the $r$ and $z$ components of the normal stress in (4.4). Although Duchesne *et al.* (2019) consider the normal stress boundary condition, they ignore this crucial viscous term and reach an erroneous conclusion.

## 5. Conclusions

Applying conservation of radial and wall-normal momentum to the flow in an expanding axisymmmetric thin film shows that the curvature of the film is singular at a finite radius determined by a critical value of the Weber number. This singularity arises from the wall-normal momentum conservation which implies that $\frac{d^2h}{dr^2} \to \infty$ whereas $(\frac{dh}{dr})^2 \to 0$ at a finite radius. Essentially the same jump condition can be obtained by applying conservation of radial momentum.

Using conservation of energy Bhagat *et al.* (2018) showed that the radial velocity gradient is also singular, in this case $\frac{dh}{dr} \to \infty$, at a critical Weber number which is numerically slightly different. This radius was identified in experiments as a jump in the flow depth to a thicker and slower flow downstream, and excellent quantitative agreement was found in the predicted and observed values of the jump radius.

There is a slight numerical difference between the two predictions with $R$ is given by

$$\frac{R}{R_{\rm ST}} = \left( \frac{1}{f'(0)(2\pi)^3} \frac{C_2}{C_1^3} \right)^{1/4} = 0.2705 \text{ and } \left( \frac{1}{f'(0)(2\pi)^3} \frac{C_3}{C_1^3} \right)^{1/4} = 0.2481,$$

by conservation of energy and momentum, respectively. These numerical values are obtained from Watson's similarity profile which, as we discuss above, do not strictly apply, and the predictions are both smaller than the experimentally measured values of $0.289 \pm 0.015$. Since $C_1$ is the area under the curve $f(\eta)$ then this will be smaller for the real profile (figure 2), leading to a larger prediction. Also, since $0 \leqslant \eta \leqslant 1$, $C_2 > C_3$, the jump radius estimate from momentum conservation is always smaller than that obtained from energy conservation.

## Acknowledgement

RKB wishes to thank his PhD supervisor Prof Ian Wilson for his advice and support.

## Appendix

Bhagat *et al.* (2018) provided a scaling relationship for the jump radius from the following three conditions: (1) that the radial flow is balanced by viscous drag, $\frac{u}{R} \sim \frac{\nu}{h^2}$, (2) continuity implies $uRh \sim Q$, and (3) the jump is surface tension dominated which implies at the jump, $We \approx 1$. However, the theoretical analysis inclusing gravity gave the condition of hydraulic jump to be $\frac{1}{We} + \frac{1}{Fr^2} = 1$, where the Froude number $Fr = u/\sqrt{gh}$. Incorporating both gravity and surface tension modifies the scaling relation (1.1) in the form,

$$R \sim R_{ST} \left[ \sqrt{\left(\frac{Q_C}{Q}\right)^2 + 2\left(\frac{Q_C}{Q}\right)} - \left(\frac{Q_C}{Q}\right) \right]^{1/4}$$

The correction to the pure surface tension radius $\left[ \sqrt{\left(\frac{Q_C}{Q}\right)^2 + 2\left(\frac{Q_C}{Q}\right)} - \left(\frac{Q_C}{Q}\right) \right]^{1/4} =$ 0.95 and 0.77, for $Q = 2Q_C$ and $10Q_C$, respectively which shows that even for $Q \sim 10Q_C$, jump is dominated by the surface tension of the liquid.

## REFERENCES

Bhagat, R. K., Jha, N. K., Linden, P. F. & Wilson, D I. 2018 On the origin of the circular hydraulic jump in a thin liquid film. *Journal of Fluid Mechanics* **851**, R5.

Bohr, T., Dimon, P. & Putkaradze, V. 1993 Shallow-water approach to the circular hydraulic jump. *Journal of Fluid Mechanics* **254**, 635–648.

Bush, J. W. M. & Aristoff, J. M. 2003 The influence of surface tension on the circular hydraulic jump. *Journal of Fluid Mechanics* **489**, 229–238.

Duchesne, A., Andersen, A. & Bohr, T. 2019 Surface tension and the origin of the circular hydraulic jump in a thin liquid film. *arXiv:1903.11495v2* .

Duchesne, A., Lebon, L. & Limat, L. 2014 Constant froude number in a circular hydraulic jump and its implication on the jump radius selection. *EPL (Europhysics Letters)* **107** (5), 54002.

Kasimov, A. R. 2008 A stationary circular hydraulic jump, the limits of its existence and its gasdynamic analogue. *Journal of Fluid Mechanics* **601**, 189–198.

Liu, X. & Lienhard, J. H. 1993 The hydraulic jump in circular jet impingement and in other thin liquid films. *Experiments in Fluids* **15** (2), 108–116.

Mathur, M., DasGupta, R., Selvi, N. R.and John, N. S., Kulkarni, G. U. & Govindarajan, R. 2007 Gravity-free hydraulic jumps and metal femtoliter cups. *Physical review letters* **98** (16), 164502.

Mohajer, B. & Li, R. 2015 Circular hydraulic jump on finite surfaces with capillary limit. *Physics of Fluids* **27** (11), 117102.

Rojas, N. O., Argentina, M., Cerda, E. & Tirapegui, E. 2010 Inertial lubrication theory. *Physical review letters* **104** (18), 187801.

Sen, U., Chatterjee, S., Crockett, J., Ganguly, R., Yu, L. & Megaridis, C. M. 2019 Orthogonal liquid-jet impingement on wettability-patterned impermeable substrates. *Phys. Rev. Fluids* **4**, 014002.

Wang, Y. & Khayat, R. E. 2019 The role of gravity in the prediction of the circular hydraulic jump radius for high-viscosity liquids. *Journal of Fluid Mechanics* **862**, 128–161.

Watson, E. J. 1964 The radial spread of a liquid jet over a horizontal plane. *Journal of Fluid Mechanics* **20** (3), 481–499.